Inorganic Chemistry

Communication

pubs.acs.org/IC

# $U_3F_{12}(H_2O)$, a Noncentrosymmetric Uranium(IV) Fluoride Prepared via a Convenient In Situ Route That Creates $U^{4+}$ under Mild Hydrothermal Conditions

Jeongho Yeon,[†] Mark D. Smith,[†] Athena S. Sefat,[‡] T. Thao Tran,[§] P. Shiv Halasyamani,[§] and Hans-Conrad zur Loye*[,†]

[†]Department of Chemistry and Biochemistry, University of South Carolina, Columbia, South Carolina 29208, United States

[‡]Materials Science and Technology Division, Oak Ridge National Laboratory, Oak Ridge, Tennessee 37831, United States

[§]Department of Chemistry, University of Houston, Houston, Texas 77204, United States

Supporting Information

**ABSTRACT:** A new noncentrosymmetric $U^{4+}$-containing fluoride, $U_3F_{12}(H_2O)$, has been synthesized via a mild hydrothermal route and its crystal structure determined by single-crystal X-ray diffraction. The material exhibits a complex three-dimensional structure that is based on $[U_6F_{33}(H_2O)_2)]^{9-}$ hexanuclear building units consisting of corner- and edge-shared $UF_8$, $UF_9$, and $UOF_7$ polyhedra. Powder second-harmonic generation (SHG) measurements revealed that the SHG efficiency for $U_3F_{12}(H_2O)$ is comparable to that of $\alpha$-$SiO_2$. Magnetic susceptibility measurements indicated that the $U^{4+}(f^2)$-containing material exhibits a singlet ground state at low temperature. IR and UV−vis reflectance spectra were obtained, and the thermal behavior was investigated by thermogravimetric analysis.

Among actinide elements, the chemistry of uranium continues to be of particular interest because of unresolved issues related to long-term nuclear waste storage and because of the interest in advanced fuel rod assemblies.[1] To date, the majority of uranium chemistry research has focused on materials containing the fully oxidized $U^{6+}$ species rather than on materials containing the reduced $U^{4+}$ species, in spite of the fact that $U^{4+}$-containing materials can exhibit not only intriguing, complex structures because of its high coordination number but also interesting magnetic and electronic behavior because of the presence of unpaired f electrons.[2] Relatively fewer materials containing $U^{4+}$ have been reported compared to $U^{6+}$-containing materials, which motivated us to explore new, facile synthetic routes to prepare materials containing $U^{4+}$ cations.

The synthesis of $U^{4+}$-containing materials can be achieved via either of two general approaches, namely, utilization of $U^{4+}$-containing precursors or the in situ creation of $U^{4+}$ from $U^{6+}$-containing precursors.[3] Although some convenient $U^{4+}$-containing precursors are available, syntheses using these precursors require synthetic conditions under which the reduced oxidation state of uranium is preserved.[3a] In the latter case, a reducing agent is necessary to complete the redox reaction, which, however, simplifies maintainance of reducing conditions during the synthesis. It is well-known that organic species, such as polyols, oxalic acid, acetate, etc., have the ability to reduce metal cations in solution.[4] We decided to apply this approach to the creation of $U^{4+}$-containing materials. We chose uranyl acetate dihydrate as a convenient starting material because it combines being a uranium source with the acetate species, a known organic reducing agent.[4b] Although several materials containing $U^{4+}$ have been reported, many of them contain mixed-valent uranium species, suggesting that controlling the uranium oxidation states during syntheses remains a challenge.[5] Herein we describe a facile synthetic route to create, in situ, $U^{4+}$ cations under acidic, mild hydrothermal conditions, which we applied toward the synthesis of a new uranium fluoride, $U_3F_{12}(H_2O)$, at relatively low temperatures. During the mild hydrothermal reaction, the $U^{6+}$ species in the uranyl acetate dihydrate was completely reduced to $U^{4+}$ cations in a dilute hydrofluoric acid environment, as evidenced by the intense green color of the products. Interestingly, we discovered that the presence of a catalytic amount of either copper metal or copper(II) salts is essential for the reduction process because in its absence only a yellow, $U^{6+}$-based solution is obtained.

In this Communication, we report on the synthesis, structure, optical characterization, and magnetic properties of the newly synthesized $U_3F_{12}(H_2O)$, which can also function as a precursor to preparing additional new $U^{4+}$-containing materials.

Single crystals of $U_3F_{12}(H_2O)$ were synthesized via a mild hydrothermal route using $UO_2(CH_3CO_2)_2{\cdot}2H_2O$, $Cu(CH_3CO_2)_2{\cdot}2H_2O$, and dilute HF. The mixture of reactants was placed into a 23 mL Teflon-lined autoclave that was closed, heated to 200 °C, held for 24 h, and cooled slowly to room temperature [see the Experimental Section in the Supporting Information (SI) for details]. Green needle crystals were obtained along with copper metal, which was selectively removed by dissolving it in concentrated $HNO_3$. The presence of copper is necessary to obtain the high-quality crystals shown in Figure 1 in nearly quantitative yield. The powder X-ray diffraction (XRD) pattern of ground single crystals is in excellent agreement with the powder pattern calculated using the single crystal data (Figure S1 in the SI). We tested other copper sources, including $Cu^0$ powder, $Cu(NO_3)_2{\cdot}2.5H_2O$, $Cu(SO_4)_2{\cdot}5H_2O$, and $CuCl_2{\cdot}2H_2O$, under the same reaction condition. In all cases,

**Received:** June 4, 2013
**Published:** July 8, 2013

   dx.doi.org/10.1021/ic401412t | *Inorg. Chem.* 2013, 52, 8303−8305

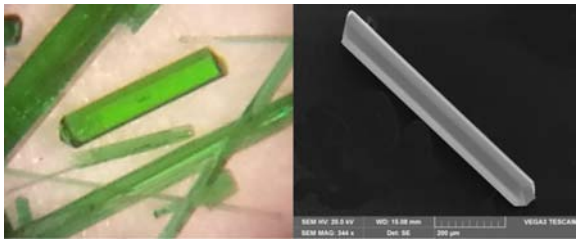

**Figure 1.** Optical (left) and scanning electron microscopy (right) images of single crystals of $U_3F_{12}(H_2O)$.

we obtained crystals and powder of $U_3F_{12}(H_2O)$. In the absence of a copper source, $U_3F_{12}(H_2O)$ could not be synthesized. Although the role of copper is unclear, we suspect that copper catalytically promotes the reduction of $U^{6+}$ to $U^{4+}$, which is essential for the formation of $U_3F_{12}(H_2O)$ crystals.

$U_3F_{12}(H_2O)$, isostructural with $Np_3F_{12}(H_2O)$,[6] crystallizes in the noncentrosymmetric monoclinic space group *Cm* and exhibits a three-dimensional crystal structure consisting of corner- and/or edge-shared $UF_8$, $UF_9$, and $UOF_7$ polyhedra (Figure 2). There are four crystallographically unique $U^{4+}$

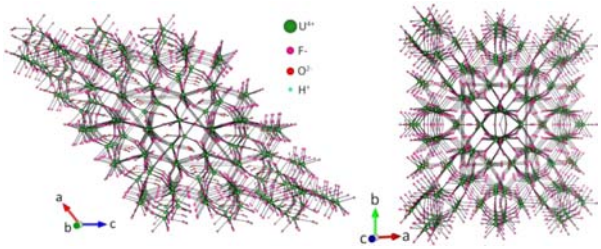


**Figure 2.** Ball-and-stick representation of $U_3F_{12}(H_2O)$ along the *b* and *c* axes.

cations, only two of which are bonded to oxygen atoms from water molecules in addition to fluorine atoms. The most interesting structural feature is the presence of the hexameric building unit, $[U_6F_{33}(H_2O)_2]^{9-}$, as shown in Figure 3. The

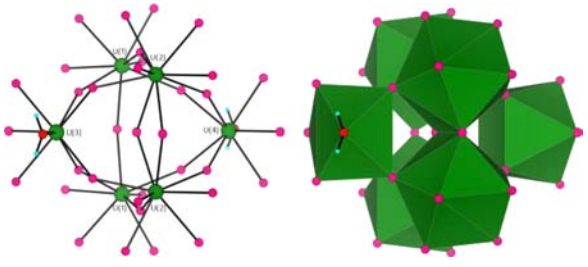

**Figure 3.** Ball-and-stick and polyhedral representation of the hexanuclear building unit $[U_6F_{33}(H_2O)_2]^{9-}$ found in $U_3F_{12}(H_2O)$.

$[U_6F_{33}(H_2O)_2]^{9-}$ units are connected to each other exclusively through fluorine atoms to build up a complex three-dimensional network. The oxygen atoms of the water molecules are bonded to the $U(3)^{4+}$ and $U(4)^{4+}$ cations, where they reside in terminal positions. In each hexamer, the $UF_8$, $UF_9$, and $UOF_7$ polyhedra are linked via corner-sharing, except for two edge-shared $U(2)F_9$ polyhedra. The $U(1)F_8$ and $U(2)F_9$ polyhedra in the hexamer contain four terminal fluorine atoms that are further connected to three $U^{4+}$ cations through two corner-sharing and one edge-sharing linkage, while the $U(3)OF_7$ and $U(4)OF_7$ polyhedra include three terminal fluorine atoms that are further linked to three $U^{4+}$ cations. As a result, each hexamer is surrounded by 18 additional $U^{4+}$ cations in all three crystallographic directions (Figure S7 in the SI), creating a complex structure. The $U(1)^{4+}$ and $U(2)^{4+}$ cations in the $U(1)F_8$ and $U(2)F_9$ polyhedra exhibit U−F bond distances of 2.246(5)−2.498(6) Å and are located in a distorted square antiprismatic and a monocapped distorted square antiprismatic coordination environment for U(1) and U(2), respectively. Both $U(3)^{4+}$ and $U(4)^{4+}$ cations are found in similar distorted square antiprismatic $UOF_7$ polyhedra, and the U−O/F bond distances range from 2.252(6) to 2.504(9) Å. The local coordination environments of all $U^{4+}$ cations are shown in Figure S7 in the SI. Bond valence sum calculations resulted in values of 4.06−4.15 for the $U^{4+}$ ion, consistent with the expected values as well as supporting the presence of the $U^{4+}$ oxidation state.

The formula of the title compound can also be written as $(UF_4)_3(H_2O)$ to emphasize the close compositional and structural relationship with $UF_4$, which can be prepared via several routes and which crystallizes in the monoclinic space group *C*2/*c*.[7] Although both materials exhibit a similar chemical composition and both are built up of hexameric building units, the individual building units are not the same. $UF_4$ is composed of $(U_6F_{38})^{14-}$ building blocks rather than the $[U_6F_{33}(H_2O)_2]^{9-}$ building blocks found in $U_3F_{12}(H_2O)$ (Figures S8 and S9 in the SI). Also, $U_3F_{12}(H_2O)$ contains corner- and edge-sharing $UF_8$, $UF_9$, and $UOF_7$ polyhedra, whereas $UF_4$ contains only corner-sharing $UF_8$ polyhedra. In addition, fewer additional $U^{4+}$ cations are bonded to the hexameric units in $U_3F_{12}(H_2O)$ because of the occurrence of edge-sharing polyhedra that are not observed in $UF_4$.

The IR spectrum for $U_3F_{12}(H_2O)$ reveals two bands around 3400 and 1600 $cm^{-1}$, which are attributable to O−H vibrations in the water molecules (Figure S2 in the SI). The bands around 650 $cm^{-1}$ are due to U−F vibrations. The UV−vis diffuse reflectance spectrum shows several absorption bands due to the f−f transition of the $U^{4+}$ cation, consistent with reports on $U^{4+}$-containing materials in the literature.[8] The band gap, estimated by the onset of the absorption edge, is 3.8 eV, indicating semiconducting behavior (Figure S3 in the SI).

The thermal behavior of $U_3F_{12}(H_2O)$ was investigated using thermogravimetric analysis (TGA) up to 900 °C under a nitrogen gas flow (Figure S4 in the SI) There are two weight loss steps observed in the TGA data, one near 350 °C and one near 800 °C. A powder XRD analysis of the residue from the 350 °C weight loss was consistent with the presence of $UF_4$ (major) and $UO_2$ (minor) (Figure S5 in the SI). This is consistent with the water molecules reacting with the uranium rather than being released intact. Consequently, the observed weight loss of 3.9% at 350 °C is likely due to the release of 2HF (calcd 4.2%) rather than the release of $H_2O$ (calcd 1.9%). Heating the material in air above 400 °C resulted in the formation of $U_3O_8$, indicating, not unexpectedly, that $U_3F_{12}(H_2O)$ oxidizes when heated in the presence of oxygen (Figure S6 in the SI).

Second-harmonic generation (SHG) measurements were performed on $U_3F_{12}(H_2O)$, as it crystallizes in a noncentrosymmetric space group (Figure S10 in the SI). Powder SHG measurement using 1064 nm radiation revealed that the SHG efficiency of $U_3F_{12}(H_2O)$ is comparable to that of $\alpha$-$SiO_2$ in the particle size range of 45−63 $\mu$m. This weak SHG efficiency is not unexpected because of small local dipole moments of 0.75−3.26 D[9] due to rather symmetrical local coordination environments, as opposed to materials that exhibit strong SHG efficiencies owing to highly asymmetric coordination environments.[10]


dx.doi.org/10.1021/ic401412t | *Inorg. Chem.* 2013, 52, 8303−8305

Additional SHG measurements with particle sizes of 20−125 $\mu$m indicated that $U_3F_{12}(H_2O)$ exhibits type 1 nonphase-matching behavior.[11]

The temperature dependence of the magnetic susceptibility for $U_3F_{12}(H_2O)$, measured in an applied field of 1000 Oe, is shown in Figure 4. No differences are found between the zero-field-cooled (zfc) and field-cooled (fc) data. The susceptibility increases gradually with decreasing temperature and begins to deviate from Curie−Weiss behavior below approximately 100 K. This deviation is ascribed to the loss of thermally accessible excited states at low temperatures and the formation of a singlet $A_1$ ground state.[3a] As shown in the inset, the inverse susceptibility data were fit to the Curie−Weiss law, $\chi = C/(T - \theta)$, where $C$ is the Curie constant and $\theta$ is the paramagnetic Weiss constant. On the basis of the linear fit in the high temperature range (100−350 K), values of 4.64 emu·K·mol$^{-1}$ and −152.9 K for $C$ and $\theta$, respectively, were extracted. From the Curie constant, the effective magnetic moment of 3.52 $\mu_B$ for the $U^{4+}$ cation was calculated, which is in excellent agreement with the theoretical value of 3.58 $\mu_B$ calculated from the Russell−Saunders coupling scheme for a $^3H_4$ ground state. As seen in Figure S11 in the SI, the $\chi_m T$ value decreases with decreasing temperature, which is consistent with the $U^{IV}$ species attaining a singlet ground state at low temperature. The $\chi_m T$ value tends toward zero below approximately 50 K with a minimum value of 0.144 emu·K·mol$^{-1}$ at 5 K. It is likely that the magnetic features at low temperature are a result of the depopulation of ligand-field levels; however, the presence of antiferromagnetic interactions cannot be ruled out, as was also observed in other known materials containing the $U^{4+}$ cations.[12]

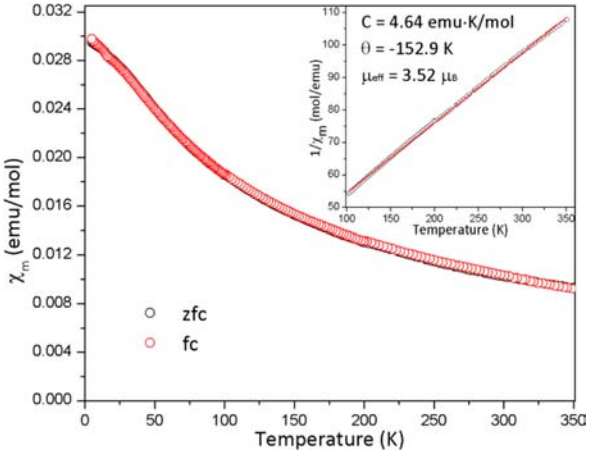


**Figure 4.** Temperature dependence of the magnetic susceptibility of $U_3F_{12}(H_2O)$ measured in an applied field of 1000 Oe. Inset: inverse susceptibility versus temperature plot with a fit to the Curie−Weiss law.

Preliminary experiments have demonstrated that $U_3F_{12}(H_2O)$ can be used effectively as a $U^{4+}$ source in the synthesis of other $U^{4+}$-containing materials. This work will be communicated by us in the near future.

In conclusion, a new uranium fluoride has been synthesized via a convenient in situ redox reaction in an acidic medium aided by copper. The crystal structure exhibits a complex three-dimensional network consisting of hexanuclear building units. The material shows only weak SHG behavior. The magnetic property measurements revealed that the $U^{4+}$ cation exhibits a nonmagnetic singlet ground state at low temperatures.

## ■ ASSOCIATED CONTENT

### Supporting Information

Experimental section, characterization and structural details including a CIF file, XRD patterns, IR and UV−vis diffuse-reflectance spectra, TGA diagram, and magnetic property data. This material is available free of charge via the Internet at http://pubs.acs.org.

## ■ AUTHOR INFORMATION

### Corresponding Author

*E-mail: zurloye@mailbox.sc.edu.

### Notes

The authors declare no competing financial interest.

## ■ ACKNOWLEDGMENTS

Research supported by the U.S. Department of Energy, Office of Basic Energy Sciences, Division of Materials Sciences and Engineering. J.Y., M.D.S., and H.-C.z.L. acknowledge DOE Award DE-SC0008664 for support. P.S.H. and T.T.T., who performed the SHG measurements, thank the Welch Foundation for support (Grant E-1457).

## ■ REFERENCES

(1) (a) Yamaji, A.; Nakano, Y.; Uchikawa, S.; Okubo, T. *Nucl. Technol.* **2012**, *179*, 309. (b) Kim, K.-T. *J. Nucl. Mater.* **2010**, *404*, 128. (c) Burns, P. C.; Olson, R. A.; Finch, R. J.; Hanchar, J. M.; Thibault, Y. *J. Nucl. Mater.* **2000**, *278*, 290.

(2) (a) Vlaisavljevich, B.; Diaconescu, P. L.; Lukens, W. L., Jr.; Gagliardi, L.; Cummins, C. C. *Organometallics* **2013**, *32*, 1341. (b) Fortier, S.; Walensky, J. R.; Wu, G.; Hayton, T. W. *J. Am. Chem. Soc.* **2011**, *133*, 11732. (c) Fortier, S.; Melot, B. C.; Wu, G.; Hayton, T. W. *J. Am. Chem. Soc.* **2009**, *131*, 15512.

(3) (a) Yeon, J.; Smith, M. D.; Sefat, A. S.; zur Loye, H.-C. *Inorg. Chem.* **2013**, *52*, 2199. (b) Liu, H.-K.; Chang, W.-J.; Lii, K.-H. *Inorg. Chem.* **2012**, *50*, 11773. (c) Nguyen, Q.-B.; Lii, K.-H. *Inorg. Chem.* **2011**, *50*, 9936. (d) Lai, Y.-L.; Chiang, R.-K.; Lii, K.-H.; Wang, S.-L. *Chem. Mater.* **2008**, *20*, 523.

(4) (a) Yeon, J.; Sefat, A. S.; Tran, T. T.; Halasyamani, P. S.; zur Loye, H.-C. *Inorg. Chem.* **2013**, *52*, 6179. (b) Piao, X.; Machida, K.-i.; Horikawa, T.; Yun, B. *J. Lumin.* **2009**, *130*, 8. (c) Kumar, L. H.; Viswanathan, B.; Murthy, S. S. *J. Alloys Compd.* **2008**, *461*, 72.

(5) (a) Diwu, J.; Albrecht-Schmitt, T. E. *Inorg. Chem.* **2012**, *51*, 4432. (b) Chen, C.-L.; Nguyen, Q. B.; Chen, C.-S.; Lii, K.-H. *Inorg. Chem.* **2012**, *51*, 7463. (c) Lin, C.-H.; Lii, K.-H. *Angew. Chem., Int. Ed.* **2008**, *47*, 8711.

(6) Cousson, A.; Gasperin, M. *Acta Crystallogr., Sect. C* **1985**, *41*, 814.

(7) (a) Larson, A. C.; Roof, R. B., Jr.; Cromer, D. T. *Acta Crystallogr.* **1964**, *17*, 555. (b) Cacciari, A.; DeLeone, R.; Fizzotti, C.; Gabaglio, M. *Energy Nucl.* **1956**, *3*, 462. Brcic, B. S.; Slivnik, J. *"J. Stefan" Inst. Rep.* **1955**, *2*, 47. Booth, H. S.; Krasny-Ergen, W.; Heath, R. E. *J. Am. Chem. Soc.* **1946**, *68*, 1969.

(8) (a) Carnall, W. T.; Liu, G. K.; Williams, C. W.; Reid, M. F. *J. Chem. Phys.* **1991**, *95*, 7194. (b) Krupa, J. C. *Inorg. Chim. Acta* **1987**, *139*, 223.

(9) (a) Debye, P. *Polar Molecules*; Chemical Catalog Company: New York, 1929. (b) Debye, P. *Phys. Z.* **1921**, *22*, 302.

(10) (a) Yeon, J.; Kim, S.-H.; Nguyen, S. D.; Lee, H.; Halasyamani, P. S. *Inorg. Chem.* **2012**, *51*, 2662. (b) Nguyen, S. D.; Yeon, J.; Kim, S.-H.; Halasyamani, P. S. *J. Am. Chem. Soc.* **2011**, *133*, 12422.

(11) Kurtz, S. K.; Perry, T. T. *J. Appl. Phys.* **1968**, *39*, 3798.

(12) (a) Siladke, N. A.; Meihaus, K. R.; Ziller, J. W.; Fang, M.; Furche, F.; Long, J. R.; Evans, W. J. *J. Am. Chem. Soc.* **2011**, *134*, 1243. (b) Nocton, G.; Pecaut, J.; Mazzanati, M. *Angew. Chem., Int. Ed.* **2008**, *47*, 3040. (c) Schelter, E. J.; Morris, D. E.; Scott, B. L.; Thompson, J. D.; Kiplinger, J. L. *Inorg. Chem.* **2007**, *46*, 5528.